VNU Journal of Science: Mathematics - Physics

Journal homepage: https://js.vnu.edu.vn/MaP

Original Article

Synthesis and Characterization of Hierarchical CeO_2 Spherical Nanoparticles for Photocatalytic Degradation of Methylene Blue

Le Huu Trinh[1,2], Nguyen Duc Cuong[1,*], Do Dang Trung[3], Nguyen Van Hieu[4]

[1]*Hue University, 77 Nguyen Hue, Phu Nhuan, Hue, Vietnam*

[2]*Ba Ria-Vung Tau College of Education, 689 Cach Mang Thang Tam, Long Toan, Ba Ria, Vietnam*

[3]*University of Fire Fighting and Prevention, Khuat Duy Tien, Thanh Xuan, Hanoi, Vietnam*

[4]*Phenikaa University, Nguyen Van Trac, Ha Dong, Hanoi, Vietnam*

Received 13 April 2021
Revised 26 April 2021; Accepted 26 April 2021

Abstract: In this study, hierarchical CeO_2 spherical nanoparticles were fabricated by the polyol method using Ceri (III) acetate hydroxide, sodium hydroxide, and triethylene glycol as precursors. The product was characterized by XRD, SEM, and TEM. The results show that the cerium oxide spherical nanoparticles built from primary nanoparticles with the average size of ~5 nm, exhibited dispersion and uniform size and shapes with their average particle diameter of ~50 nm in size. With such a good morphology, CeO_2 material possessed good catalytic activity for the decomposition of methylene blue (MB), in which the material was synthesized at a hydrothermal temperature of 80 ^oC (CeO_2-80) for the best MB decomposition performance.

Keywords: CeO_2, hierarchical nanostructure, polyol method, photocatalyst, methylene.

1. Introduction

Cerium dioxide (CeO_2), one of the most important compounds of rare earth elemental materials, is attracting a lot of research interest because of its unique physical and chemical properties, low cost, and abundance. To date, CeO_2 nanomaterial has been a promising candidate for a variety of application scopes, such as gas sensor [1], catalyst [2], environmental treatment [3] and biomedicine [4], etc. It is

* Corresponding author.
E-mail address: nguyenduccuong@hueuni.edu.vn

https//doi.org/10.25073/2588-1124/vnumap.4646

known that the unique properties of CeO_2 nanostructures relate significantly to their morphology, particle size, and surface defect [5-7]. Thus, various CeO_2 nanostructures including nanorods, nanowires [8], nanoparticles [9], nanocubes [10], nanotubes [11] and so on have been synthesized by many different approaches. Among diverse CeO_2 nanostructures, the hierarchical nanostructures, that are assembled from the lower-dimensional, have attracted considerable attention because of their high porosity, large specific surface area, and less agglomerated configuration [12]. For example, the hierarchical CeO_2 nanotube exhibited a superior catalytic property for CO oxidation in comparison with CeO_2 nanoparticles [13]. The 3D hierarchical CeO_2 nanospheres showed high catalytic activity of toluene oxidation due to their large surface area and hierarchical porous structure, which possesses abundant surface oxygen vacancies [14]. Therefore, the development of simple, low-cost chemical methods for the synthesis of hierarchical CeO_2 nanostructures with high uniformity and dispersion, always receives the attention of researchers to explore new properties of the material for critical applications.

Polyol is considered to be an important synthetic strategy for the preparation of nanoparticles with control of size, morphology, and composition with high crystallinity. After about three decades of development, the polyol method is now widely recognized as a unique chemical method for the preparation of large numbers of nanoparticles for use in important technological areas. This method has many advantages such as low cost, ease of use, and, more importantly, scalability on an industrial scale [14]. Ho et al. used the polyol method to successfully synthesize CeO_2 nanorods and nanospindles by control of the duration of reaction and concentration of cerium precursor [15]. Cheng et al. reported a simple polyols-mediated solvothermal approach to preparing CeO_2 microcrystals with tunable morphologies [16]. Soren et al. prepared CeO2 nanoparticles with narrow size distribution by microwave mediated polyol method in just 10 min [17]. Recently, our group has developed a rapid polyol route with microwave assistance to fabricate uniform Gd_2O_3 nanoparticles with the control of particle size. However, the application of the polyol method to synthesize the hierarchical CeO_2 nanostructures with high uniformity and dispersion has not been published.

In this work, we presented a facile polyol method to prepare the hierarchical CeO_2 nanospheres using triethylene glycol (TEG) as a surfactant. The obtained nanomaterial showed a uniform spherical shape with good dispersion, which was assembled from primary nanoparticles with the diameter of ~5 nm. Furthermore, the hierarchical CeO_2 nanospheres exhibited excellent catalytic activity for the methylene blue (BM) decomposition reaction.

2. Experiment

2.1. Materials

All chemicals were used as received from providers without further purification. Cer*ium* (III) *acetate* hydrate ($Ce(CH_3CO_2)_3{\cdot}xH_2O$ – 99,9%) was purchased from AK Scientific; sodium hydroxide (NaOH - 99,99%) and triethylene glycol ($HO(CH_2)_2O(CH_2)_2$ $O(CH_2)_2OH$ – 99%) were purchased from Merck.

2.2. Preparation of CeO_2 Nanoparticles

In a typical procedure, 1.2 g of $Ce(CH_3CO_2)_3{\cdot}xH_2O$ and 20 ml of triethylene glycol was dissolved completely in 200 ml double distilled water in a 500 mL beaker. The reaction mixture was magnetically stirred at 60 ^oC for 4 h to obtain a homogeneous solution. Subsequently, drop by drop of 19 mL of 0.05 M NaOH solution was added to the above reaction mixture. The reaction was performed at 80 ^oC for 3 h. The solution's color transfers from colorless to a whitish color. The product was filled, washed,

and then dried in a thermometer at 125 °C for 14 h. The obtained product possesses light yellow powder, which was annealed at 600 °C for 3 h to obtain CeO_2 nanomaterials. To investigate the effect of hydrothermal temperature on the CeO_2 nanomaterials' morphology, the reaction was carried out at various temperatures including 70, 80, and 90 °C. The as-synthesized CeO_2 nanomaterials were named as CeO_2-70, CeO_2-80 and CeO_2-90 for 70, 80 and 90 °C, respectively.

2.2. Photocatalytic Tests

The photocatalytic activity of hierarchical CeO_2 nanospheres was carried out in the degradation reaction of MB under UV light (20W, 365 nm) at ambient temperature. In a photoreaction experiment, 50 mg of the CeO_2 nanomaterial was added in a conical flask that contained 100 mL of varying concentrations of MB (5, 10, 15, and 20 ppm). Before irradiation, the mixture was stirred in the dark for 60 min to reach the MB adsorption/desorption equilibrium. At certain time intervals, about 5 mL of the reaction solution was withdrawn and then the residual nanocatalyst was removed for analysis by using a UV-Visible spectrophotometer (Jasco V-550 UV-Vis). The absorption intensity of MB at 667 nm was used to determine the concentration of MB according to the duration of reaction, where C_0 and C_t are the initial concentration of MB and concentration of MB at any time of the photocatalytic process, respectively.

2.3. Material Characterization

The products were characterized by X-ray diffraction (XRD, D8 Advance, Brucker, Germany) with Cu K_α (λ = 1.5406 nm) radiation and TGA (STA 409PC, Netzsch). The morphology and the average particle size of CeO_2 nanostructures were investigated via scanning electron microscopy (SEM, Model JSM-5300LV) and transmission electron microscopy (TEM, Model JEOLE-3432, Japan). The nitrogen adsorption/desorption isotherms of the heat-treated samples were obtained using Micromeritics at 77 K. The Brunauer-Emmett-Teller (BET) specific surface areas (S_{BET}) were calculated using the BET equation. Desorption isotherm was used to determine the pore size distribution using the Barret-Yoyner-Halender (BJH) method.

3. Results and Discussion

3.1. Characterization of Hierarchical CeO_2 Nanospheres

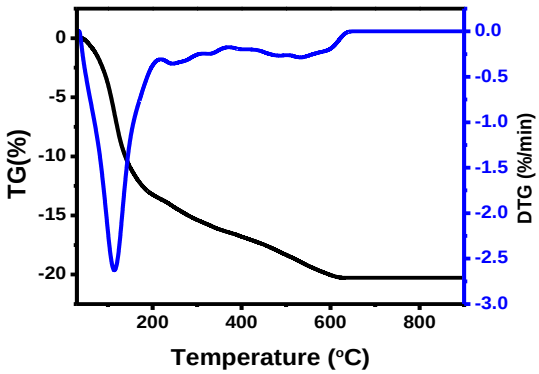

Figure 1. TG and DTG curves of as-synthesized CeO_2 nanoparticle precursor.

The thermo-decomposition behavior of the precursor of CeO_2-80 sample was measured by TG analysis as shown in Figure 1. From the TG curve, it is seen that the first weight loss, of 13.72 % between 75 and 250 ^oC (endothermic peak at 114.06 ^oC), corresponds to the removal of the residual water in the sample and the water was weakly adsorbed to the surface of the nanoparticles [18, 19]. The second weight loss, of 6.55% occurring between 250 and 650 ^oC (endothermic peak at 248.54 ^oC and 533.49 ^oC), corresponds to the removal of TEG (boiling point 285 ^oC) in the sample, complete oxidation process of TEG and organic compounds' remnants of the oxidation process. The TG results indicated that 600 ^oC is a suitable calcination temperature when no significant weight loss was observed in the TG profile after 600 ^oC.

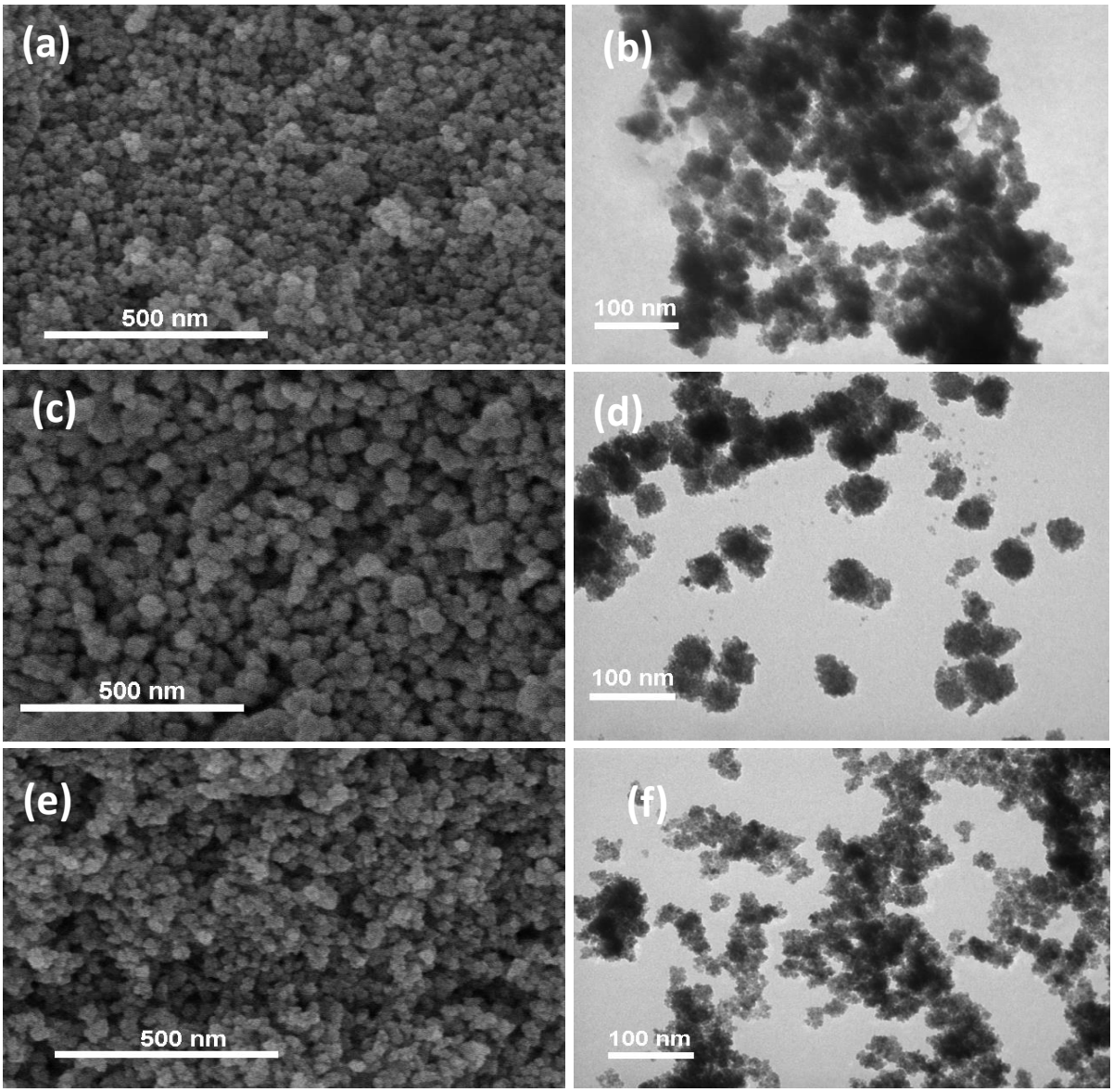

Figure 2. SEM and TEM images of CeO_2-70 (a, b), CeO_2-80 (c, d) and CeO_2-90 (e, f).

The effect of reaction temperature on the morphology of as-prepared CeO_2 nanocrystals was investigated. The SEM and TEM images in Figure 2 indicate that the morphology of the nanocrystal can be tuned through the control of reaction temperature. At all hydrothermal temperatures (70-90 ^oC), the obtained CeO_2 nanomaterials possess a hierarchical structure with spherical shapes and regular dispersion. The hierarchical architecture was assembled from primary nanoparticles that were about 5 nm in diameter. The SEM and TEM results indicate that the CeO_2 NPs synthesized at 80 ^oC are the best dispersion and narrow particle size distribution .

The formation of the CeO_2 spherical nanoparticles may occur in a two-stage reaction process, involving the synthesis of primary nanoparticles according to reactions (1), (2), and (3) [5] after the aggregation of the primary particles to form spherical nanostructures [20].

$$4Ce^{3+}(aq) + O_2(aq) + 4OH^- + 2H_2O \leftrightarrow Ce(OH)_2^{2+} \quad (1)$$

$$Ce(OH)_2^{2+}(aq) + 2OH^- \leftrightarrow Ce(OH)_4(s) + 2H_2O \quad (2)$$

$$Ce(OH)_4 \leftrightarrow CeO_2 + 2H_2O \quad (3)$$

The XRD pattern of the CeO_2-80 sample was carried out to identify crystalline phases and to estimate the crystalline sizes (Figure 3). Figure 3 shows the XRD of hierarchical CeO_2-80 nanospheres. The peaks correspond to the (111), (200), (311), (222), (331) of cubic face-centered structure of CeO_2 (JCPDS No, 00-034- 0394, a = b = c = 5.41134 A^0).

To determine the grai size (τ) we used Sherrer's foumular as follows [21]:

$$\tau = \frac{0.9\lambda}{\beta.\cos\theta}, \quad (4)$$

where λ is X-ray wavelength, β is the full width at half maximum in radians and θ is the Bragg angle of the considered diffraction peak. The average crystalline size of ceria nanoparticles calculated from the XRD data is about 5 nm.

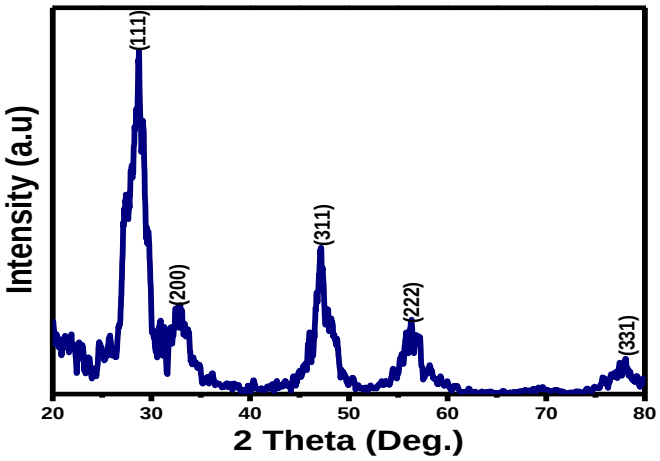

Figure 3. XRD patterns of the hierarchical CeO_2-80 nanospheres.

FT-IR spectra of the CeO_2-80 and the precursor of the CeO_2-80 sample were analyzed to better understand the chemical nature of the products (Figure 3). As seen in Figure 4a, the calcined sample

exhibited bands characteristic of cubic CeO_2 at 433 cm^{-1} which were assigned to Ce–O stretching modes that indicate the formation of CeO_2 [22]. The typical absorption bands of CO_3^{2-} at 850 and 1056 cm^{-1} and gaseous CO_2 at 1307 and 2366 cm^{-1} can be observed because H_2O and CO_2 molecules are chemisorbed easily on the CeO_2 surface when they are exposed to the atmosphere [23]. Besides, the peak at 3419 cm^{-1} was attributed to –OH group of water. In Figure 4b, the peaks at 2926 and 2868 cm^{-1} correspond to the symmetric and asymmetric stretching vibration of $–CH_2–$ in TEG capping the CeO_2. The peak at 1112 cm^{-1} is related to TEG chain C-O-C stretching vibration, and the peaks at 1378 and 1562 cm^{-1} are attributed to symmetric and asymmetric stretching vibration of COO^- [24]. The presence of the COO^- group resulted from partial oxidation of polyol TEG at $–CH_2–OH$ group during synthesis at high temperature. Compared with calcined CeO_2, the Ce–O stretching band of as-synthesized CeO_2 nanoparticles shifts to 445 cm^{-1}, demonstrating that cerium ions bind to the COO^- group of TEG.

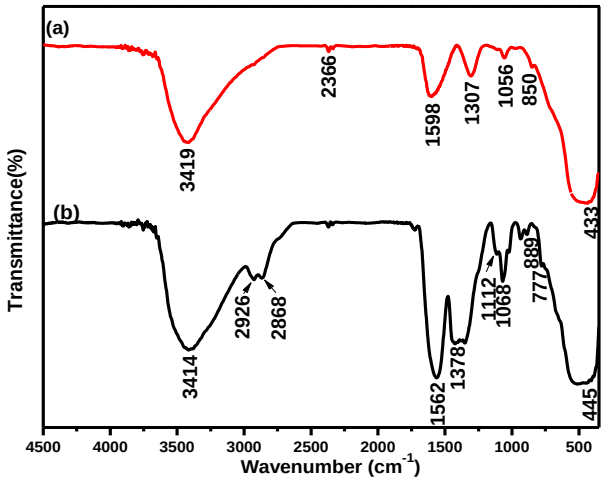

Figure 4. FT-IR spectra of (a) calcined CeO_2-80 and (b) respective CeO_2-80 nanoparticle precursor.

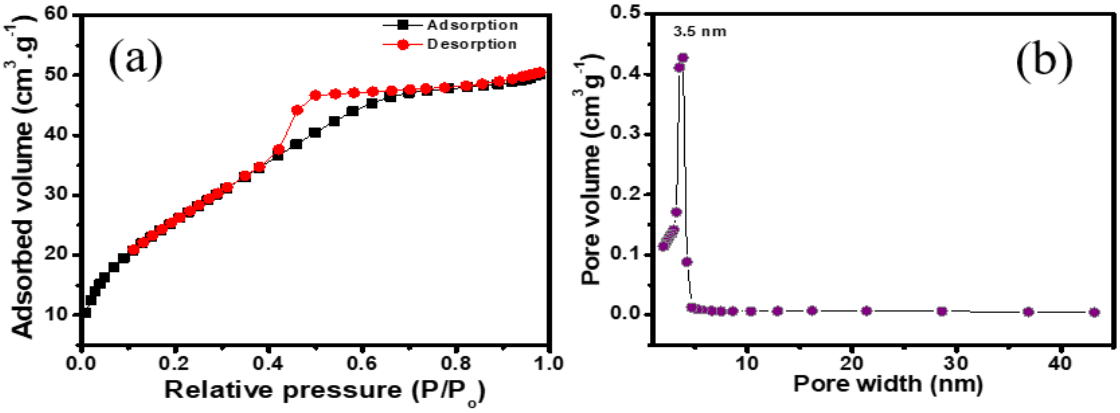

Figure 5. N_2 absorption-desorption isotherm (a) and BHJ pore size distribution (b) of hierarchical CeO_2-80 nanospheres.

The textural characterization of hierarchical CeO_2 nanospheres was determined by nitrogen adsorption-desorption as shown in Figure 5. The isotherm curves (Figure 5a) show type IV with H_3 hysteresis loop, which confirms the presence of mesoporous structure in the obtained CeO_2 nanomaterial with a narrow average pore diameter [25]. The material has a very high specific surface area of 99.57 m^2/g. Figure 5b indicates that the materials possess a homogeneous pore system with narrow pore size distribution and average pore size of 3.5 nm. The hierarchical CeO_2 nanospheres with high surface area and narrow pore size distribution can contribute to new catalytic properties.

3.2. The Photocatalytic Activity of the Hierarchical CeO_2 Nanomaterials

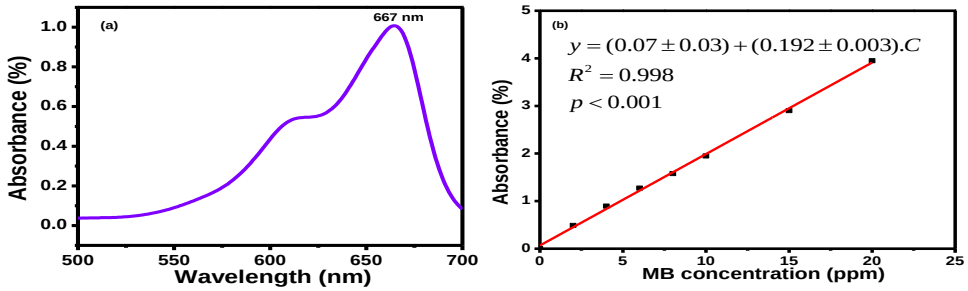

Figure 6. (a) UV-vis absorption spectra of MB solution (5 ppm) and (b) the absorption intensity at λ_{max} versus MB concentration.

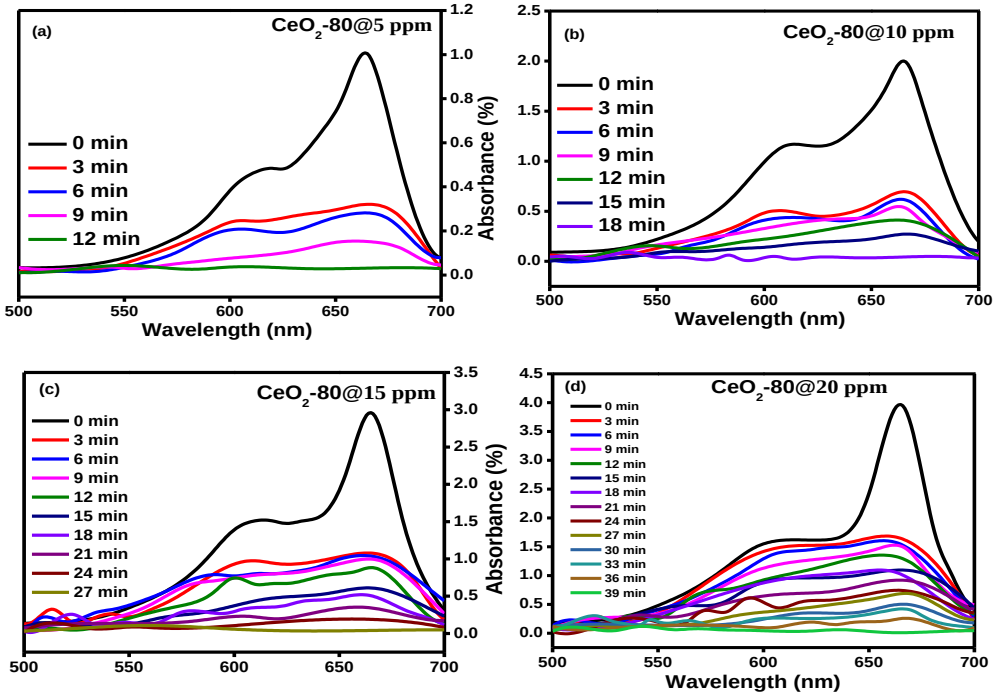

Figure 7. UV-Vis spectra curves of different MB concentrations versus time under UV irradiation of CeO_2-80 nanocatalysts: (a) 5 ppm, (b) 10 ppm, (c) 15 ppm, and (d) 20 ppm.

To characterize the photocatalytic activity of the prepared CeO_2 nanomaterials, we used the photodegradation reaction of methylene blue (MB) under UV irradiation. Figure 6a shows the UV-vis absorption spectra of MB solution (5 ppm). It can be found that the maximum absorption wavelength of MB (λ_{max}) is ~667 nm. With the concentration of MB range of 5-20 ppm, the absorption intensity at 667 nm exhibited as a linear function of MB concentration (Figure 6b). Thus, four concentrations of MB include 5 ppm, 10 ppm, 15 ppm, and 20 ppm were used to test the photocatalytic properties of CeO_2 nanomaterials.

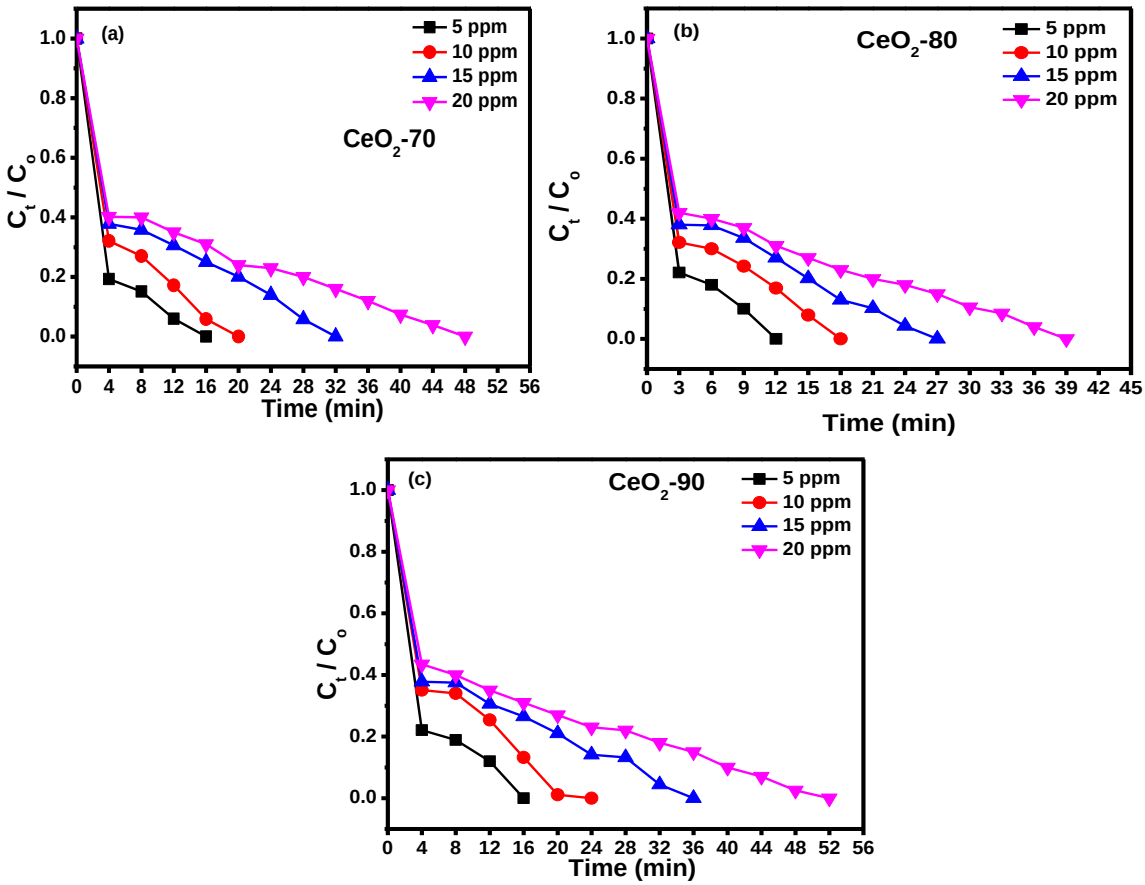

Figure 8. The photodegradation of MB versus time using different catalysts: (a) CeO_2-70, (b) CeO_2-80 and (c) CeO_2-90.

The photocatalytic properties of the hierarchical CeO_2 nanospheres (CeO_2-80) were tested with different concentrations of MB (5 ppm, 10 ppm, 15 ppm, and 20 ppm) as shown in Figure 7. As can be seen in Figure 7, the absorption intensity of MB increases quickly in all concentrations of MB. With MB concentration of 5ppm, the characteristic absorption of MB disappeared with an irradiation time of just 12 min. The decomposition rate of MB decreases significantly with the increase of MB concentration. The decomposition times are 18, 27, and 39 min for 10, 15, and 20 ppm of MB, respectively. The results can be explained by several effects: i) The penetration of the light into the reaction solution was restricted when the MB concentration increased; and ii) The increase of

MB molecules adsorbed on the surface of CeO_2 catalyst that prevented the generation of hydroxyl radicals [26, 27].

The photocatalytic properties of CeO_2-70 and CeO_2-90 were also investigated and compared with the CeO_2-80 sample, which was presented in Figure 8. The results indicate that the time needed for complete degradation of MB increased gradually with CeO_2-70 and CeO_2-90 catalysts in comparison with CeO_2-80 catalyst. Meanwhile, the respective degradation time of 20 ppm MB for CeO_2-70, CeO_2-80, and CeO_2-90 is 48, 39 and 52 min. The enhancement of the photocatalytic activity of uniform hierarchical CeO_2 nanospheres may relate to unique architecture, which can generate more active sites due to its high specific surface area and narrow pore size distribution.

4. Conclusion

In this work, the uniform hierarchical CeO_2 nanospheres were successfully synthesized by the polyol method. The hierarchical nanospheres with a particle size of 50 nm were assembled from primary CeO_2 nanoparticles with an average diameter of 5 nm. The nanomaterial possesses a large surface area of 99.57 m^2/g with a narrow pore distribution. The heterogeneous CeO_2 nanomaterials show excellent photocatalytic activity for degradation reaction of MB under UV irradiation, which is critical for practical applications.

Acknowledgments

This work was supported by the National Foundation for Science and Technology Development (NAFOSTED) under Grant 103.02-2018.21.

References

[1] D. N. Oosthuizen, D. E. Motaung, H. C. Swart, Gas Sensors Based on CeO_2 Nanoparticles Prepared by Chemical Precipitation Method and Their Temperature-Dependent Selectivity Towards H_2S and NO_2 Gases, Appl. Surf. Sci, Vol. 505, 2020, pp. 144356, https://doi.org/10.1016/j.apsusc.2019.144356.

[2] K. Polychronopoulou, M. A. Jaoudé, Nano-Architectural Advancement of CeO_2-Driven Catalysis via Electrospinning, Surf. Coatings Technol, Vol. 350, 2018, pp. 245-280, https://doi.org/10.1016/j.surfcoat.2018.07.014.

[3] C. Sun, H. Li, L. Chen, Nanostructured Ceria-Based Materials: Synthesis, Properties, and Applications, Energy Environ. Sci, Vol. 5, 2012, pp. 8475, https://doi.org/10.1039/c2ee22310d.

[4] B. Nelson, M. Johnson, M. Walker, K. Riley, C. Sims, Antioxidant Cerium Oxide Nanoparticles in Biology and Medicine, Antioxidants, Vol. 5, No. 2, 2016, pp. 15, https://doi.org/10.3390/antiox5020015.

[5] L. T. T. Tuyen, D. Q. Khieu, H. T. Long, D. T. Quang, C. T. L. Trang, T. T. Hoa, N. D. Cuong, Monodisperse Uniform CeO_2 Nanoparticles: Controlled Synthesis and Photocatalytic Property, J. Nanomater, Vol. 2016, 2016, pp. 8682747, https://doi.org/10.1155/2016/8682747.

[6] M. Piumetti, S. Bensaid, T. Andana, M. Dosa, C. Novara, F. Giorgis, N. Russo, D. Fino, Nanostructured Ceria-Based Materials: Effect of the Hydrothermal Synthesis Conditions on the Structural Properties and Catalytic Activity, Catalysts, Vol. 7, No. 6, 2017, pp. 174, https://doi.org/10.3390/catal7060174.

[7] N. D. Cuong, D. T. Quang, Progress Through Synergistic Effects of Heterojunction in Nanocatalysts - Review, Vietnam J. Chem, Vol. 58, No. 4, 2020, pp. 434-463, https://doi.org/10.1002/vjch.202000072.

[8] Z. Ji, X. Wang, H. Zhang, S. Lin, H. Meng, B. Sun, S. George, T. Xia, A. E. Nel, J. I. Zink, Designed Synthesis of CeO_2 Nanorods and Nanowires for Studying Toxicological Effects of High Aspect Ratio Nanomaterials, ACS Nano, Vol. 6, No. 6, 2012, pp. 5366-5380, https://doi.org/10.1021/nn3012114.

[9] H. Cai, W. Jing, S. Guo, L. Liu, Y. Ye, Y. Wen, Y. Wu, S. Wang, X. Huang, J. Zhang, Effects of Micro/Nano CeO_2 on The Microstructure and Properties of WC-10Co Cemented Carbides, Int. J. Refract. Met. Hard Mater, Vol. 95, 2021, pp. 105432, https://doi.org/10.1016/j.ijrmhm.2020.105432.
[10] L. Zhang, J. Zhang, Y. Huang, H. Xu, X. Zhang, H. Lu, K. Xu, P. K. Chu, F. Ma, Stability and Sensing Enhancement by Nanocubic CeO_2 with {100} Polar Facets on Graphene for NO_2 at Room Temperature, ACS Appl. Mater. Interfaces, Vol. 12, No. 4, 2020, pp. 4722-4731, https://doi.org/10.1021/acsami.9b18155.
[11] D. Zhang, H. Fu, L. Shi, J. Fang, Q. Li, Carbon Nanotube Assisted Synthesis of CeO_2 Nanotubes, J. Solid State Chem, Vol. 180, No. 2, 2007, pp. 654-660, https://doi.org/10.1016/j.jssc.2006.11.025.
[12] R. S. Anzorena, F. F. Muñoz, P. Bonelli, A. L. Cukierman, S. A. Larrondo, Hierarchical, Template-free Self-Assembly Morphologies in CeO_2 Synthesized via Urea-hydrothermal Method, Ceram. Int, Vol. 46, No. 8, 2020, pp. 11776-11785, https://doi.org/10.1016/j.ceramint.2020.01.212.
[13] J. Huang, C. Wang, L. Jin, F. Chen, Z. Chen, Synthesis of Biomorphic Hierarchical CeO_2 Microtube with Enhanced Catalytic Activity, Trans. Nonferrous Met. Soc. China, Vol. 27, No. 3, 2017, pp. 578-583, https://doi.org/10.1016/S1003-6326(17)60064-5.
[14] Z. Feng, M. Zhang, Q. Ren, S. Mo, R. Peng, D. Yan, M. Fu, L. Chen, J. Wu, D. Ye, Design of 3-Dimensionally Self-Assembled CeO_2 Hierarchical Nanosphere as High Efficiency Catalysts for Toluene Oxidation, Chem. Eng. J, Vol. 369, 2019, pp. 18-25, https://doi.org/10.1016/j.cej.2019.03.051.
[15] C. Ho, J. C. Yu, T. Kwong, A. C. Mak, S. Lai, Morphology-controllable Synthesis of Mesoporous CeO_2 Nano- and Microstructures, Chem. Mater, Vol. 17, No. 17, 2005, pp. 4514-4522, https://doi.org/10.1021/cm0507967.
[16] G. Cheng, J. Xiong, F. J. Stadler, A Facile Polyol-mediated Approach to Tunable CeO_2 Microcrystals and Their Photocatalytic Activity, Powder Technol. Vol. 249, 2013, pp. 89-94, https://doi.org/10.1016/j.powtec.2013.07.033.
[17] S. Soren, M. Bessoi, P. Parhi, A Rapid Microwave Initiated Polyol Synthesis of Cerium Oxide Nanoparticle using Different Cerium Precursors, Ceram. Int, Vol. 41, No. 6, 2015, pp. 8114-8118, https://doi.org/10.1016/j.ceramint.2015.03.013.
[18] P. Chen, F. Q. Zhao, Y. Luo, R. Z. Hu, S. W. Li, Y. Gao, Thermal Decomposition Kinetics of Triethylene Glycol Dinitrate, Chinese J. Chem, Vol. 22, No. 10, 2010, pp. 1078-1082, https://doi.org/10.1002/cjoc.20040221005.
[19] A. L. Nuzhdin, G. A. Bukhtiyarova, P. E. Plyusnin, A. A. Porsin, V. I. Bukhtiyarov, Effect of Mono-, Di-, and Triethylene Glycol on the Sulfidation Behavior of $NiMo(P)/Al_2O_3$ Hydrotreating Catalysts, Catal. Letters, Vol. 149, 2019, pp. 3304-3311, https://doi.org/10.1007/s10562-019-02898-1.
[20] L. H. Trinh, D. Q. Khieu, H. T. Long, T. T. Hoa, D. T. Quang, N. D. Cuong, A Novel Approach for Synthesis of Hierarchical Mesoporous Nd_2O_3 Nanomaterials, J. Rare Earths, Vol. 35, No. 7, 2017, pp. 677-682, https://doi.org/10.1016/S1002-0721(17)60963-3.
[21] N. D. Cuong, T. T. Hoa, D. Q. Khieu, T. D. Lam, N. D. Hoa, N. V. Hieu, Synthesis, Characterization, and Comparative Gas-Sensing Properties of Fe_2O_3 Prepared from Fe_3O_4 and Fe_3O_4-Chitosan, J. Alloys Compd, Vol. 523, 2012, pp. 120-126, https://doi.org/10.1016/j.jallcom.2012.01.117.
[22] C. Xu, X. Qu, Cerium Oxide Nanoparticle: A Remarkably Versatile Rare Earth Nanomaterial for Biological Applications, NPG Asia Mater. Vol. 6, 2014, pp. e90, https://doi.org/10.1038/am.2013.88.
[23] S. Kumar, A. K. Ojha, Ni, Co and Ni–Co Codoping Induced Modification in Shape, Optical Band Gap and Enhanced Photocatalytic Activity of CeO_2 Nanostructures for Photodegradation of Methylene Blue Dye under Visible Light Irradiation, RSC Adv, Vol. 6, 2016, pp. 8651-8660, https://doi.org/10.1039/C5RA14184B.
[24] L. H. Trinh, T. T. Hoa, N. V. Hieu, N. D. Cuong, Facile Synthesis of Ultrafine Gd_2O_3 Nanoparticles by Polyol Microwave Method, J. Electron. Mater, Vol. 46, No. 6, 2017, pp. 3484-3490, https://doi.org/10.1007/s11664-017-5480-2.
[25] P. L. Quang, N. D. Cuong, T. T. Hoa, H. T. Long, C. M. Hung, D. T. T. Le, N. V. Hieu, Simple Post-Synthesis of Mesoporous P-Type Co_3O_4 Nanochains for Enhanced H_2S Gas Sensing Performance, Sensor. Actuat. B, Vol. 270, 2018, pp. 158-166, https://doi.org/10.1016/j.snb.2018.05.026.
[26] L. Yan, R. Yu, J. Chen, X. Xing, Template-Free Hydrothermal Synthesis of CeO_2 Nano-octahedrons and Nanorods: Investigation of the Morphology Evolution, Cryst. Growth Des, Vol. 8, No. 5, 2008, pp. 1474-1477, https://doi.org/10.1021/cg800117v.
[27] R. Dhanabal, A. Chithambararaj, S. Velmathi, A. C. Bose, Visible Light Driven Degradation of Methylene Blue Dye using Ag_3PO_4, J. Environ. Chem. Eng, Vol. 3, No. 3, 2015, pp. 1872-1881, https://doi.org/10.1016/j.jece.2015.06.001.